AE-185
UDC 621.039.512.4
621.039.538

AE-185

A New Method for Predicting the Penetration and Slowing-Down of Neutrons in Reactor Shields

L. Hjärne and M. Leimdörfer

AKTIEBOLAGET ATOMENERGI
STOCKHOLM, SWEDEN 1965

A NEW METHOD FOR PREDICTING THE PENETRATION AND SLOWING-DOWN OF NEUTRONS IN REACTOR SHIELDS

L. Hjärne and M. Leimdörfer

Abstract

A new approach is presented in the formulation of removal--diffusion theory. The "removal cross-section" is redefined and the slowing-down between the multigroup diffusion equations is treated with a complete energy transfer matrix rather than in an age theory approximation. The method, based on the new approach, contains an adjustable parameter. Examples of neutron spectra and thermal flux penetrations are given in a number of differing shield configurations and the results compare favorably with experiments and Moments Method calculations.

Printed and distributed in May 1965

LIST OF CONTENTS

1. Background

It is well recognized that the diffusion approximation of the Boltzmann transport equation provides considerable advantages in the numerical work required to solve neutron transport problems. An implicit assumption of diffusion theory is, however, that the Legendre modes of the angular flux of order higher than one can be neglected. Such an approximation is not justified in shielding problems, where the flux at deep penetrations is made up of neutrons which have undergone strongly forward-peaked collisions and thus contains many high-order Legendre components. An attempt to improve the diffusion approximation for such problems is made by the introduction of the "removal-diffusion" method which is a combination of diffusion theory with a separate treatment of the high-order flux components. The most extensively used model of the physical situation is built on the assumption that the high-order flux terms can be represented collectively by a virgin flux, attenuated by a cross-section somewhat smaller than the total cross-section. This "uncollided" flux is called the removal flux and the attenuating cross-section is the removal cross-section. The numerical calculation of the removal flux may be carried out in an energy-dependent fashion by dividing the fission source spectrum into energy groups or points. The ways of introducing the removal flux into diffusion theory vary. The simplest approach is to calculate the total collision density, corresponding to the removal flux, assign a typical energy to the neutrons coming out of collisions (say 2 MeV), and insert this source into the highest-energy group in a series of multigroup diffusion equations [1, 2, 3]. The great virtue of this model is its simplicity. The drawbacks are the facts that the removal cross-section has to be determined largely on an empirical basis and that the coupling of the removal flux into the diffusion equations is too rough to permit a good fast neutron spectrum to be obtained.

The theory that we shall present here profits from the experience obtained when using the older methods, but this approach contains a new development of the removal technique. We hope that the development of the new formalism, as compared to the earlier ones, will shed some light on the physics behind the "removal-diffusion" techniques.

2. Description of the method

We start this outline at the fission process and discreticize the continuous energy spectrum of the neutrons released in fission to an array of δ-functions distributed systematically over the energy interval containing fission neutrons. (A finite-width energy band structure may also be conceived.) The density of "spikes" is considered sufficiently large for accurate representation of the fission spectrum.

The flux of neutrons having suffered no collision or only strongly forward-directed collisions, for historical reasons hereafter referred to as the removal flux, denoted $\phi(\bar{r}, E_i)$, may be calculated by integration of an uncollided kernel $K_i(\bar{r}, \bar{r}')$ over the core volume with a properly defined removal cross-section $\Sigma_{rem}(E_i)$. E_i are the fission spectrum discretization points. Let us set the number of fission neutrons released per unit volume equal to $q(\bar{r}', E_i)$. Then

$$\phi(\bar{r}, E_i) = \int_{\substack{\text{core} \\ \text{volume}}} K_i(\bar{r}, \bar{r}')\, q(\bar{r}', E_i)\, d\bar{r}' \qquad (1)$$

where

$$K_i(\bar{r}, \bar{r}') = \frac{\exp\left\{-\left[\left|\bar{r} - \bar{r}'\right| \Sigma_{rem}(E_i)\right]\right\}}{4\pi \left|\bar{r} - \bar{r}'\right|^2} \qquad (2)$$

for the homogeneous case, the generalization to the heterogenous case being trivial. In doing this, we rely on the postulate that the neutrons which have suffered small-angle deviations encounter a Σ_{rem} at the energy at which they were released.

We define $\Sigma_{rem}(E_i)$ by the relation

$$\Sigma_{rem}(E_i) = \Sigma_{tot}(E_i) - 2\pi \int_{-1}^{1} w(\mu) \Sigma_{el}(E_i, \mu) d\mu \qquad (3)$$

where $w(\mu)$ is a weight function. Strictly speaking, the weight function should also be dependent upon position and energy. It should be defined as the function which produces the correct sum of the contributions to the scalar flux from the higher-order ($\ell > 1$) modes of a break-up of the

solution of the Boltzmann equation into spherical harmonics (disregarded in the diffusion equation) obtained by integration of eq. (2). We rely on the experience gained from earlier removal methods when assuming that the weight function is independent of position and energy. A mathematical justification of this assumption can be obtained only by comparison with results obtained from rigorous transport theory. We have chosen to set $w(\mu) = \begin{cases} 0; \mu < \mu_o \\ 1; \mu \geq \mu_o \end{cases}$. The parameter μ_o is the cosine of an angle, in the center-of-mass* system of reference, defining a cone into which the virgin neutrons may be scattered without losing their character of being (virtually) unscattered. To maintain the physical meaning of the energy points E_i, it is desirable that the energy degradation coupled to the deviation μ_o is not stronger than that the neutrons are kept above the next lower energy point E_{i+1}. The strongest energy degradation is, of course, obtained with a hydrogen moderator, having the scattering law $\mu = 2\frac{E}{E'} - 1$ (μ is the center-of-mass cosine). This gives the condition

$$\mu_o > 2\frac{E_{i+1}}{E_i} - 1 \qquad (4)$$

The constant μ_o will be the only adjustable parameter of our formalism.

The criterion for validity of our model is equivalent to the question whether it is possible to obtain correct results, i. e. neutron spectra and thermal fluxes. The fact that this was indeed possible, gives justification to our model. An interpretation of μ_o in terms of rigorous transport theory would strengthen our arguments; this has not yet been possible but some effort is being devoted to this end. The optimum value of the constant μ_o in the search was 0.6 (see below). With the energy point structure (E_i) used in our removal flux calculation, the value of E_{i+1}/E_i was constant and equal to 0.794 (cf. eq. (4)). This means that, to take the extreme case, a neutron assigned to the energy point E_i might actually have an energy that has

---

* In an earlier description [14] of this method μ_o has erroneously been said to be the laboratory angle.

decreased to $0.8 \cdot E_i$ by a collision with hydrogen. This choice of parameters does not inflict the inequality (4).

To throw light on the effect of removal "energy overlap" we modified our energy point representation to a smoothed-out multigroup structure (in which case the effect of "energy overlap" should be more obvious than before). To simplify our notation we define a group averaging operator $\mathcal{G}_{\Psi G}$:

$$\mathcal{G}_{\Psi G} f(E) = \frac{\int_{E_G}^{E_{G-1}} \Psi(E) f(E) dE}{\int_{E_G}^{E_{G-1}} \Psi(E) dE} \tag{5}$$

where $\Psi(E)$ is a first guess of the shape of the removal flux within the group G ($E_{G-1} > E_G$). This "removal spectrum" can be assumed to be rather unchanged within an energy group throughout the shield, and consequently the fission spectrum should be an acceptable guess. We average eq. (3) over the group G:

$$\Sigma_{rem,G} = \mathcal{G}_{\Psi G} \Sigma_{rem}(E) \tag{6}$$

The removal fluxes are fitted as source terms into a multigroup diffusion scheme by the operation

$$S = C \cdot \Phi \tag{7}$$

where Φ is a removal flux vector, the elements of which are the energy point or group values of the integral of $K_i(\bar{r}, \bar{r}')$ over the source volume. S is a vector of removal source terms in the diffusion equations and C a conversion matrix. The matrix elements give the number of neutrons that are transferred from removal group i to diffusion group g by elastic and inelastic collisions per unit length

$$c_{ig} = \int_{E_g}^{E_{g-1}} \Sigma_{el}\left[E_i, \mu(E)\right] dE + \int_{E_g}^{E_{g-1}} \Sigma_{in}(E_i, E) dE \tag{8a}$$

In the smoothed-out version the matrix elements are defined by

$$c_{Gg} = \mathcal{J}_{\Phi G} c_g(E) \tag{8b}$$

where

$$c_g(E) = \int_{E_g}^{E_{g-1}} \Sigma_{el}\left[E, \mu(E, E')\right] dE' + \int_{E_g}^{E_{g-1}} \Sigma_{in}(E, E') dE' \tag{8c}$$

The difference in final results between the two methods, represented by eqs. (3), (8a) and eqs. (6), (8b), (8c), respectively, was small or none and hence the effect of removal energy overlap is negligible. The general expressions appearing in eqs. (8a) and (8c) contain elastic scattering angular distributions and inelastic scattering energy distributions. The physical meaning of equations (7) and (8a, b, c) is that we calculate the number of neutrons that come out of a "first" collision and distribute them into the energy groups of the diffusion equations according to their expected energy distribution. The angular distribution of these removal sources is taken as uniform, which is the inherent assumption of diffusion theory. A detailed account of the treatment of cross-section data is given below.

We now proceed to discussing the diffusion theory part. The energy dependent diffusion equation may be written

$$D(E)\Delta\varphi(\bar{r}, E) - \Sigma_{abs}(E)\varphi(\bar{r}, E) + \int \Sigma(E' \to E)\varphi(\bar{r}, E') dE' + Q(\bar{r}, E) = 0 \tag{9}$$

where the scattering kernel is the same as in the transport equation. $Q(\bar{r}, E)$ is the sum of the external sources and "removal" sources.

By integrating eq. (9) over an energy band g with upper and lower bounds E_{g-1} and E_g, respectively, we obtain the multigroup diffusion equations:

$$D_g \Delta\varphi_g(\bar{r}) - \Sigma_{abs,g}\varphi_g(\bar{r}) + \sum_{g'} \Sigma_{g' \to g}\varphi_{g'}(\bar{r}) + Q_g(\bar{r}) = 0 \tag{10}$$

where

$$\varphi_g(\bar{r}) = \int_{E_g}^{E_{g-1}} \varphi(\bar{r}, E)dE$$

We now proceed to the definitions of the multigroup constants in eq. (10) assuming separability of the scalar flux in space and energy (cf. [4]). We use the operator in eq. (5), now with an assumed shape, φ, of the neutron flux within the group g. Consequently, the group constants are defined as follows:

$$D_g = \mathcal{G}_{\varphi g} D(E) \tag{11}$$

(The usual auxiliary assumptions in diffusion theory permit us to shift the order of D_g and the Δ operator in eq. (9) as well as in eq. (10)).

$$\Sigma_{abs,g} = \mathcal{G}_{\varphi g}\left\{\Sigma(E) - \int_{E_g}^{E_{g-1}} \Sigma(E\to E')dE'\right\} \tag{12}$$

$$\Sigma_{g\to g'} = \mathcal{G}_{\varphi g} \int_{E_{g'}}^{E_{g'-1}} \Sigma(E\to E')dE \tag{13}$$

The loss of neutrons due to real absorption ((n, γ), (n, p), (n, α)-reactions etc.) is obviously given by

$$(\Sigma_{abs,g} - \sum_{g'} \Sigma_{g\to g'})\,\varphi_g \tag{14}$$

The general expressions for $\Sigma_{g\to g'}$ are rather complicated. The scattering cross-section $\Sigma(E\to E')$ can be divided into an elastic part Σ_{el} and an inelastic part Σ_{in}, the latter containing also reactions like (n, 2n), (n, np), and also fission may be contained in this part. For the elastic scattering part we obtain the expression

$$\Sigma_{g\to g',el} = \mathcal{G}_{\varphi g}\left\{\Sigma_{el}(E)\sum_{\ell} \frac{2\ell+1}{2} f_\ell(E) \int_{g'} P_\ell(\mu)d\mu\right\} \tag{15}$$

where P_ℓ and f_ℓ are the ℓth Legendre polynomial and coefficient, respectively.

$$\Sigma_{el}(E,\mu) = \frac{\Sigma_{el}(E)}{2\pi}\sum_{\ell}\frac{2\ell+1}{2} f_\ell(E)P_\ell(\mu) \quad \text{(in barns/ster.)} \qquad (16)$$

The integration symbol in eq. (15) stands for one of the alternatives:

$$0, \int_{-1}^{\mu(E_{g'-1})}, \int_{\mu(E_{g'})}^{\mu(E_{g'-1})}, \int_{\mu(E_g)}^{1}, \text{ and } \int_{-1}^{1}$$

either of the last two being used only when we compute the $\Sigma_{abs,g}$. $\mu = \mu(E')$ can be obtained from

$$\left(\alpha = \left(\frac{A-1}{A+1}\right)^2 \leq\right) \frac{E'}{E} = 1 - \frac{2A}{(A+1)^2}(1-\mu) \left(= 1 - \tfrac{1}{2}(1-\alpha)(1-\mu) \leq 1\right) \qquad (17)$$

Solving the integral in eq. (15) we make use of the formula

$$\int_{-1}^{\mu} P_\ell(\mu')d\mu' = \frac{1}{2\ell+1}\left\{P_{\ell+1}(\mu) - P_{\ell-1}(\mu)\right\} \qquad (18)$$

and get

$$\Sigma_{g\to g',el} = \mathcal{J}_{\varphi g}\left\{\tfrac{1}{2}\Sigma_{el}(E)\sum_{\ell=0}^{L}(f_{\ell-1} - f_{\ell+1})\left[P_\ell(\mu_1) - P_\ell(\mu_o)\right]\right\} \qquad (19)$$

after rearranging the summation. $f_\ell = 0$ for $\ell = -1$ and for $\ell > L$. μ_1 and μ_o are the upper and lower limits, given by eq. (17), of the region of integration in eq. (15).

Our treatment of inelastic scattering is different in the lower energy (discrete level) region and in the higher energy (overlapping level) region. The equality in eq. (17) will now take the form (discrete levels):

$$\frac{E'}{E} = 1 - \frac{2A}{(A+1)^2}\left(1 - \mu\sqrt{1 - \frac{A+1}{A}\cdot\frac{\varepsilon}{E}} - \frac{A+1}{2}\cdot\frac{\varepsilon}{E}\right) \qquad (20)$$

where ε is the inelastic energy loss in the c. m. system. For lower energy inelastic scattering we write $\Sigma_{in} = \sum_k \Sigma_k$ where k is the index of a nuclear excitation level corresponding to an energy loss ε_k, and $0 < \varepsilon_1 < \varepsilon_2 \ldots\ldots$ For the kth level eq. (15) will now turn into:

$$\Sigma_{g \to g', k} = \mathcal{G}_{\varphi g} \left\{ \Sigma_k(E) \sum_\ell \frac{2\ell+1}{2} f_\ell^{(k)}(E) \int_{g'} P_\ell(\mu) d\mu \right\} \tag{21}$$

where the integration region is properly redefined according to eq. (20). $f_\ell^{(k)}(E)$ is defined according to

$$\Sigma_k(E,\mu) = \frac{\Sigma_k(E)}{2\pi} \sum_\ell \frac{2\ell+1}{2} f_\ell^{(k)}(E) P_\ell(\mu) \tag{22}$$

(in barns/ster., $f_o^{(k)} = 1$ for all k). Available data indicate, however, that in general inelastic scattering is rather isotropic, and angular distribution Legendre series can be truncated after few (most often only one) terms, and therefore an acceptable approximation can be a rectangular distribution in the interval between $\alpha(E - \varepsilon)$ and $E - \varepsilon$, except in the nearest vicinity of the respective levels of the rest nucleus, but the contributions from these regions are rather small. In the higher energy region, where the levels are overlapping, an evaporation model has been applied. We use a formula based on the model of Newton [5] :

$$\Sigma(E \to E') = \left\{ \Sigma_{nn'}(E) + \Sigma_{n2n}(E) \right\} \frac{a_1 E'}{E - \delta_1} e^{-E\sqrt{\frac{a_1}{E - \delta_1}}} +$$

$$+ \Sigma_{n2n}(E) \frac{a_2 E'}{E - \delta_2 - B} e^{-E'\sqrt{\frac{a_2}{E - \delta_2 - B}}} \tag{23}$$

a_1 and a_2 are the constants in the expressions for the nuclear temperatures of the rest (not the compound) nuclei, δ_1 and δ_2 are the pairing corrections and, finally, B is the (n, 2n) threshold energy. All the quantities in eq. (23) are given in the laboratory system including B, which can be obtained from the Q-value as $B = Q \cdot (A+1)/A$. The parameters

needed in eq. (23) were taken from [5] or from measurements, where possible (e. g. [6]).

In previous removal-diffusion methods the slowing-down between diffusion groups was handled according to age theory (cf. [7]). This implies that the neutrons may be said to travel down in energy through each consecutive energy group. For hydrogen, age theory is an unsatisfactory approximation. For heavy moderating atoms the connection between our method and the older ones may be derived. Assuming the collision density $\Sigma(E)\varphi(E)$ proportional to $1/E$, the group averaging operator in eq. (5) becomes after transformation into lethargy, $u = \ln \frac{E_o}{E}$,

$$\mathcal{G}_{\text{leth, g}} f(u) = \frac{1}{\Delta u_g} \int_{u_{g-1}}^{u_g} f(u)du \tag{24}$$

where $\Delta u_g = u_g - u_{g-1}$. If the groups are wide enough we can get from eq. (15) in the case of solely elastic scattering:

$$\Sigma_{g \to g+1} = \frac{1}{\Delta u_g} \int_{-1}^{1} \frac{\Sigma_{el}(u) \sum_{\ell} \frac{2\ell+1}{2} f_\ell \int_{-1}^{\mu} P_\ell(x)dx}{\mu + \frac{1+\alpha}{1-\alpha}} d\mu \tag{25}$$

The above assumption about the collision density is equivalent to the assumption of a constant $\Sigma(E) = \Sigma_g$ within the group and the weight function $\varphi(E) \sim 1/E$. This gives in eq. (25):

$$\Sigma_{g \to g+1} = \frac{\Sigma_g}{\Delta u_g} \left\{ \tfrac{1}{2} \int_{-1}^{1} \frac{\mu + 1}{\mu + \frac{1+\alpha}{1-\alpha}} d\mu + \sum_{\ell \geq 1} \tfrac{1}{2} f_\ell \int_{-1}^{1} \frac{P_{\ell+1} - P_{\ell-1}}{\mu + \frac{1+\alpha}{1-\alpha}} d\mu \right\} \tag{26}$$

The solutions of these integrals are given as Legendre functions of the second kind (see e. g. [8])

$$(-1)^n Q_n\left(\tfrac{1+\alpha}{1-\alpha}\right) = \tfrac{1}{2} \int_{-1}^{1} \frac{P_n(\mu)}{\mu + \frac{1+\alpha}{1-\alpha}} d\mu \tag{27}$$

Inserting (27) and (26) gives

$$\Sigma_{g\to g+1} = \frac{\Sigma_g}{\Delta u_g}\left\{1 + \frac{\alpha}{1-\alpha}\log\alpha - \sum_{\ell\geq 1}(-1)^{\ell} f_{\ell}\left[Q_{\ell+1}\left(\frac{1+\alpha}{1-\alpha}\right) - Q_{\ell-1}\left(\frac{1+\alpha}{1-\alpha}\right)\right]\right\} \tag{28a}$$

which can be expressed as a series expansion in terms of the inverted atomic weight number $\gamma = \frac{1}{A}$:

$$\Sigma_{g\to g+1} = \frac{\Sigma_g}{\Delta u_g}\left\{1 + \frac{\alpha}{1-\alpha}\log\alpha - 2f_1\gamma\left(1 - \frac{1}{5}\gamma^2\ldots\right) + \frac{4}{3}f_2\gamma^2\left(1 - \frac{2}{7}\gamma^2\ldots\right) - \frac{16}{15}f_3\gamma^3 + \ldots\right\}, \tag{28b}$$

Starting from age theory, equation (28a) would read (cf. [9])

$$\Sigma_{g\to g+1} = \frac{\Sigma_g}{\Delta u_g}\cdot\xi \text{ , with}$$
$$\xi = 1 + \frac{\alpha}{1-\alpha}\ln\alpha \tag{29}$$

It is evident that the two expressions (28b) and (29) are equal when $\gamma\to 0$, i. e. for infinitely heavy moderators.

A system of computer programs, based on the method described above, has been developed for the Ferranti Mercury Computer. Translation to the FORTRAN language is in progress and it is anticipated that an IBM 7090 version will be available in the near future.

The first program in the system, NECO, provides cross-section data which are manufactured by the operations discussed above. The raw data of measured and theoretically predicted cross-sections are filed in a comprehensive library, stored in the computer during the calculation. The removal source calculation is carried out by the programs REFUSE or REBOX that work in one-dimensional plane geometry and rectangular box geometry, respectively. The diffusion theory program is called NEDI and works in one-dimensional plane, spherical, or cylindrical geometries, respectively. The running time for a complete shield is of the order of 3 - 3.5 hours on the Ferranti Mercury which corre-

sponds to less than 15 minutes on the IBM 7090. This includes the preparation of parameters with NECO. The parameters can be reused, however, in which case the computation time is reduced by about 50 per cent. A thorough description of these programs is given in [10].

3. Applications

As was mentioned above, test runs were performed on a large variety of problems to investigate the existence of a fitting value of the parameter μ_o [11]. The common trend of this analysis was that the value of μ_o did not affect the shape of the neutron spectrum but that the absolute magnitudes increased with decreasing values of μ_o. This tendency was not unexpected. In figs. 1 and 2 we show the result of comparing thermal flux calculations with experimental data. The measurements were performed at the R2-0 reactor at Studsvik, Sweden, and the two geometries presented here were taken from a comprehensive study, comparing our theoretical results with measurements [12, 13, 14]. In fig. 1 the attenuating medium is water and in fig. 2 magnetite concrete. In both cases, calculations were performed with $\mu_o = 0.5$, 0.6, and 0.7, respectively. As seen, the value $\mu_o = 0.6$ gives the best fits, but the other values give results that do not depart by more than a factor of two from the best fit even after penetrations of 180 cm in water and 140 cm in magnetite concrete, respectively. The underestimate of the predictions near the core is due to the difficulties in the interpretation of the geometry [12]. It is interesting to note that the thermal fluxes for different values of μ_o coincide at small distances from the core. This fact indicates that the removal source does not contribute to the source term in the thermal group diffusion equation near the core. In water, the critical penetration distance seems to be about 60 cm. This observation is consistent with the well-known fact that diffusion theory works rather well when applied to thermal reactor criticality problems.

In fig. 3 we show the results of a comparison of theory and experiment in a laminated geometry of iron and heavy water [13]. The quantities compared are the mean epithermal flux per unit lethargy

(0.1 eV - 100 eV) and sulfur activation, respectively. The value of μ_o was 0.6.

In fig. 4 we show the result of a calculation of the neutron spectrum made by our method in the water geometry of fig. 1 at a point 120 cm from the core face. A Moments Method [15] calculation for the corresponding water penetration in point source geometry is shown for comparison and the agreement is excellent. μ_o was set equal to 0.6.

Fig. 5 shows a spectrum in the concrete geometry of fig. 2, calculated at 30 cm concrete penetration. Our results ($\mu_o = 0.6$) are compared with a NIOBE (Numerical Integration of the Boltzmann Equation [16]) calculation in the same geometry and with the same cross-section data. (The computer time needed for a NIOBE run is about 10 - 20 times longer than for our method.) The agreement is very good above 1 keV, but the NIOBE spectrum has a stronger slope than 1/E at lower energies. Our results have a 1/E shape which is more like one would expect. The discrepancy may be ascribed to a known interpolation difficulty in the NIOBE program.

Lately it was reported [11] that values of $\mu_o = 0.60$ for $A > 1$ and $\mu_o = 0.45$ for hydrogen give a still better fit to experimental data.

4. Conclusions

The method presented here for treating the penetration and slowing-down of neutrons in radiation shields gives good results over the whole energy range from 18 MeV and downwards. The fact that it was possible to adjust the parameter involved so that the results agree with experimental data justifies the assumptions made.

References

1. AVERY A F et al.
Methods of calculation for use in the design of shields for power reactors.
1960. (AERE-R 3216).

2. PETERSON E G
MAC - a bulk shielding code.
1962. (HW-73381).

3. FOWLER A G
Bendix G-20 computer programs for use in reactor shield design.
1962. (AECL-1678), (CRRP-1127).

4. POMRANING G C
On the energy averaging of the diffusion coefficient.
Nucl. Sci. & Eng. 19 (1964) 249.

5. NEWTON T D
Shell effects on the spacing of nuclear levels.
Can. J. of Phys. 34 (1956) 804.

6. THOMSON D B
Nuclear level densities and reaction mechanisms from inelastic neutron scattering.
Phys. Rev. 129 (1963) 1679.

7. WEINBERG A M and WIGNER E P
The physical theory of neutron chain reactors.
Chicago. Univ. of Chicago Press, 1958, p. 376.

8. JAHNKE, EMDE, LÖSCH
Tables of higher functions.
Stuttgart, Teubner, 1960, p. 111.

9. GLASSTONE S and EDLUND M C
The elements of nuclear reactor theory.
Princeton. N. J. Van Nostrand, 1952, p. 157.

10. HJÄRNE L (ed.)
A user's manual for the NRN shield design method.
1964 (AE-145).

11. AALTO E, FRÄKI R and MALÉN K
The fine-adjustment of the neutron penetration in the NRN-method.
(To be published in Nucl. Sci. & Eng.).

12. AALTO E and NILSSON R
Measurements of neutron and gamma attenuation in massive laminated shields of concrete and a study of the accuracy of some methods of calculation.
1964. (AE-157).

13. AALTO E
Comparisons of measured and calculated neutron fluxes in laminated iron and heavy water.
(Nucl. Sci. & Eng., in press).

14. AALTO E, HJÄRNE L, and LEIMDÖRFER M
A new shield design method and some attenuation studies in laminated biological shields.
To be published in Proc. of the 3rd Conf. on the Peaceful Uses of Atomic Energy, Geneva 1964. (A/CONF. 28/P/684).

15. GOLDSTEIN H
Fundamental aspects of reactor shielding.
Reading, Mass., Addison-Wesley, 1958, p. 265.

16. YETMAN D et al.
Military compact reactor program. Description of input preparation and operating procedures for 9-NIOBE, an IBM-7090 code.
1961. (NDA 2143-18).

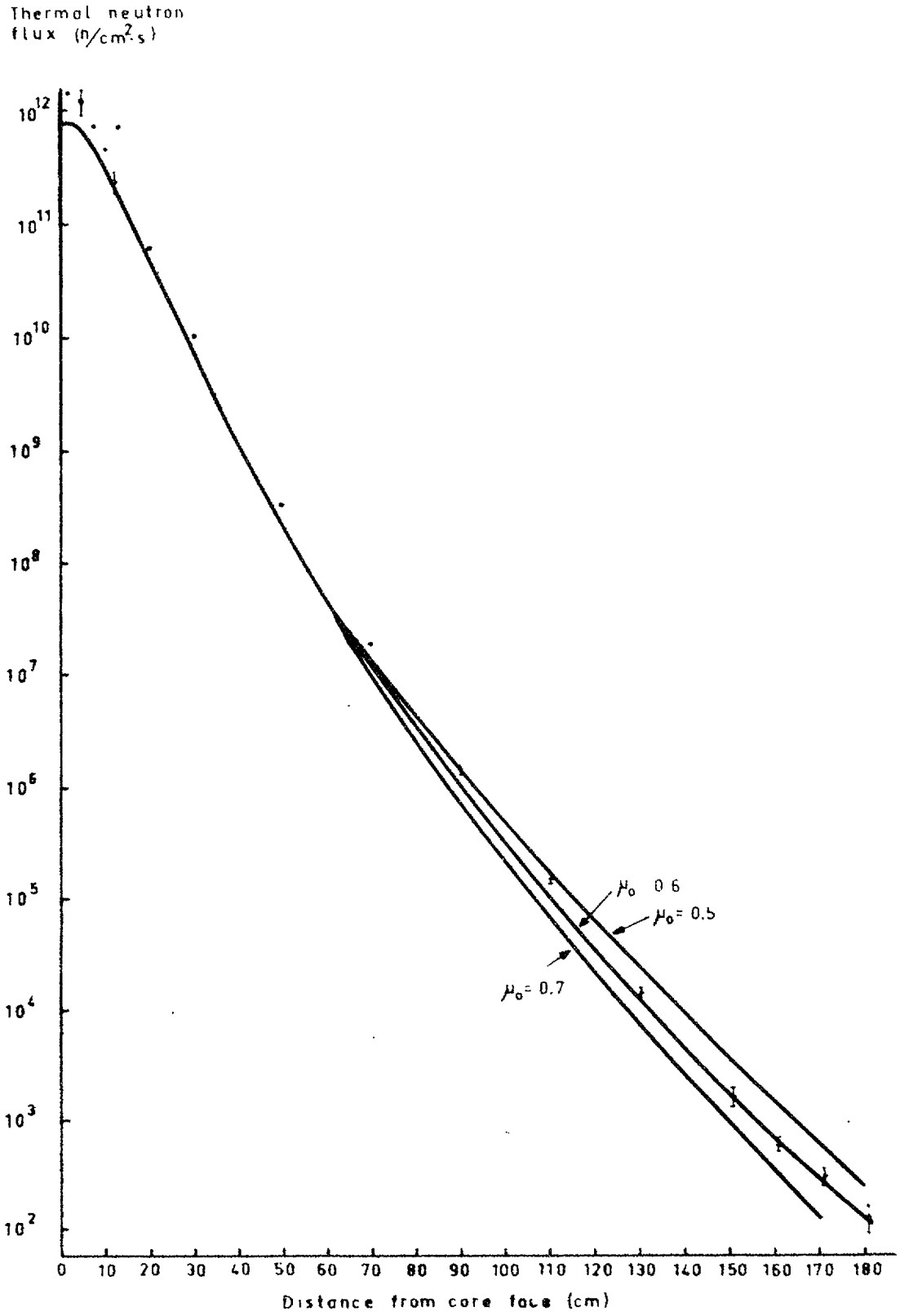

Fig. 1. Calculations and measurements of the thermal flux in the water pool of the R2-0 reactor. The three curves represent values of μ_o = 0.5, 0.6, and 0.7, respectively. The underestimate of the predictions near the core is due to an inconsistency in the interpretation of the geometry.

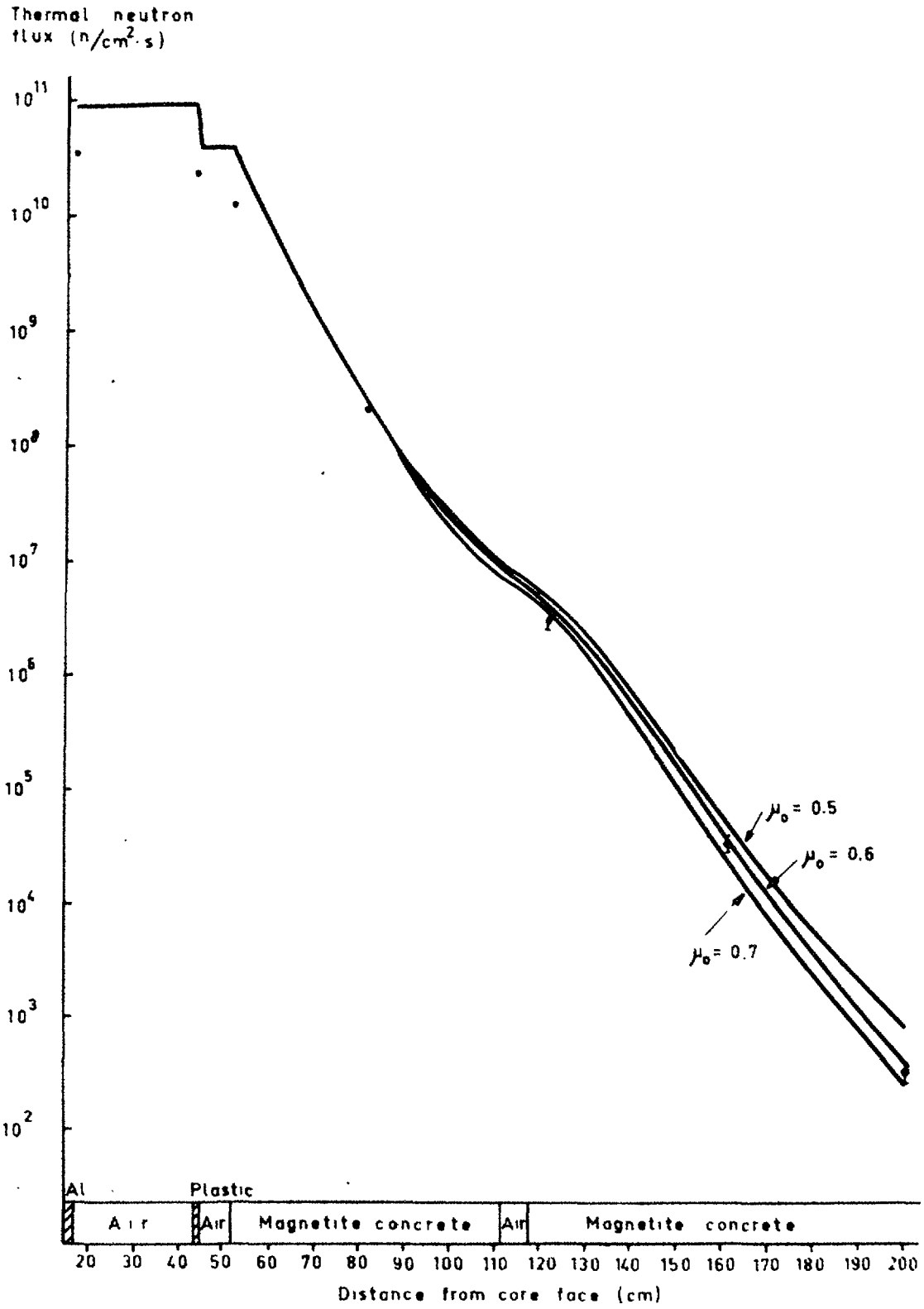

Fig. 2. Calculations and measurements of the thermal flux in a shielding experiment performed at the R2-0 reactor. The low experimental values in the air gaps may be due to transverse neutron leakage. The three curves represent values of μ_o = 0.5, 0.6, and 0.7, respectively. The underestimate of the predictions near the core is due to an inconsistency in the interpretation of the geometry.

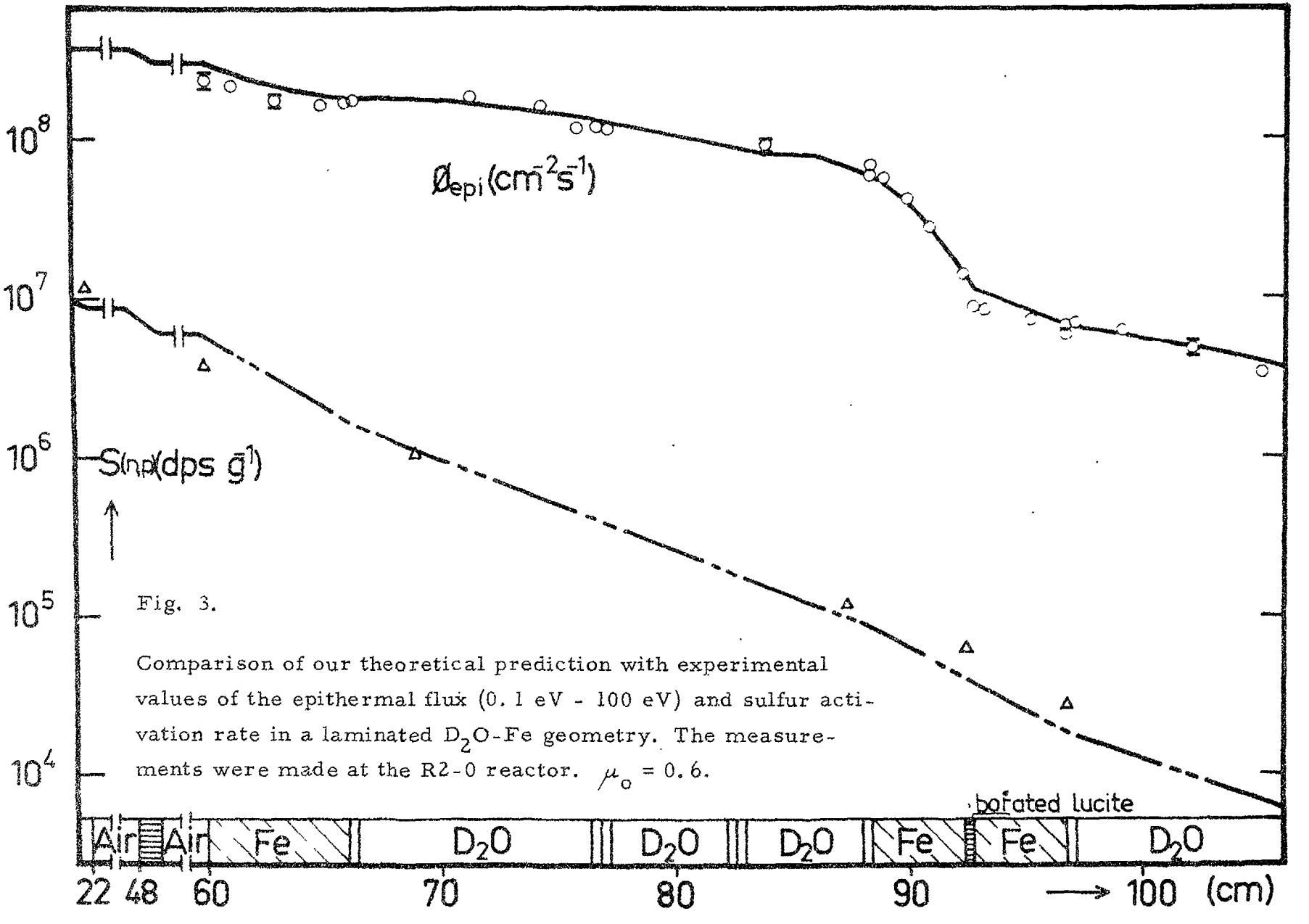

Fig. 3.

Comparison of our theoretical prediction with experimental values of the epithermal flux (0.1 eV - 100 eV) and sulfur activation rate in a laminated D_2O-Fe geometry. The measurements were made at the R2-0 reactor. $\mu_o = 0.6$.

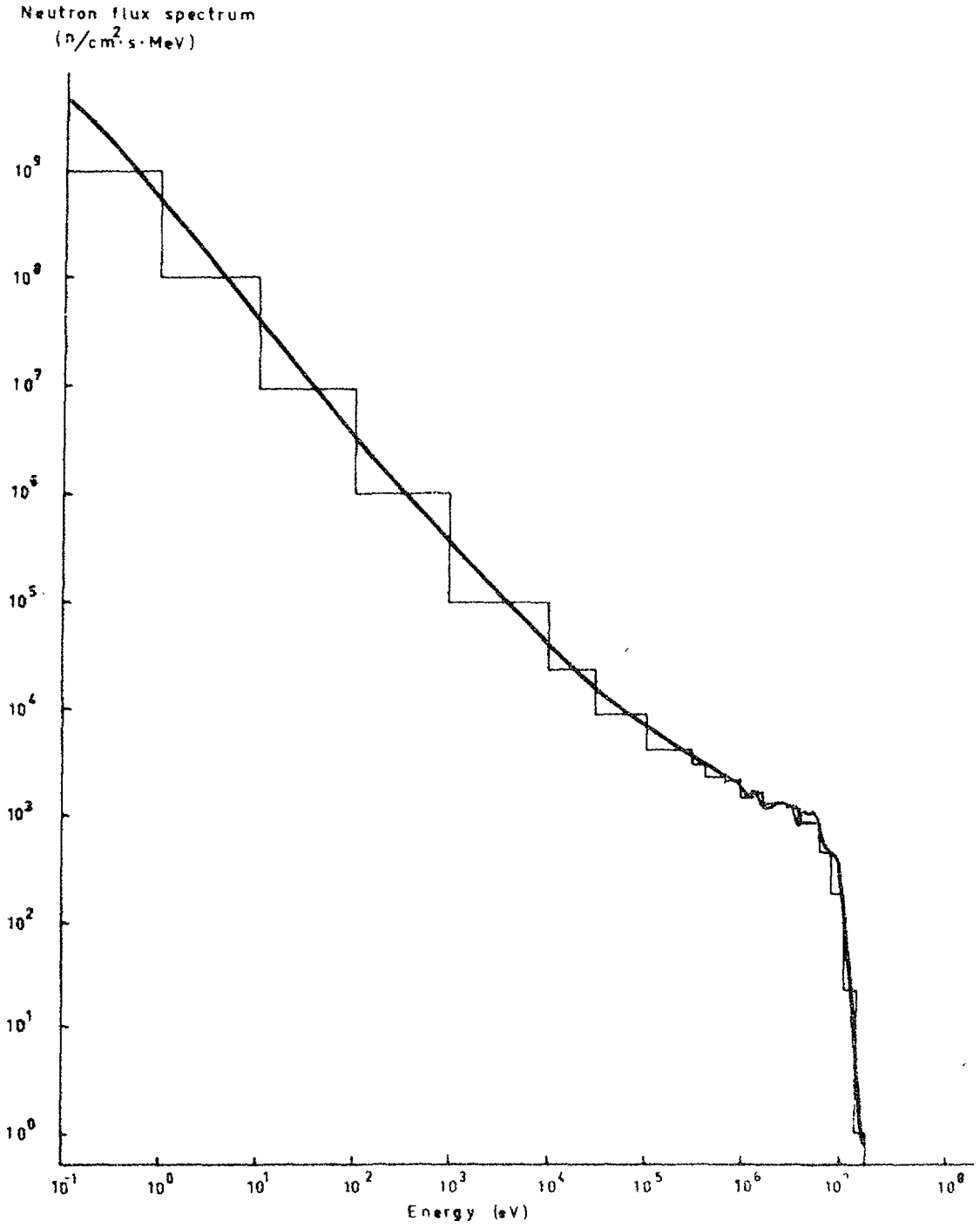

Fig. 4. Neutron flux spectrum at 120 cm in the geometry of fig. 1. Our theoretical prediction (histogram) is compared to a Moments Method calculation (curve) in point (fission) source geometry, normalized to the correct neutron source strength and water penetration distance. $\mu_o = 0.6$.

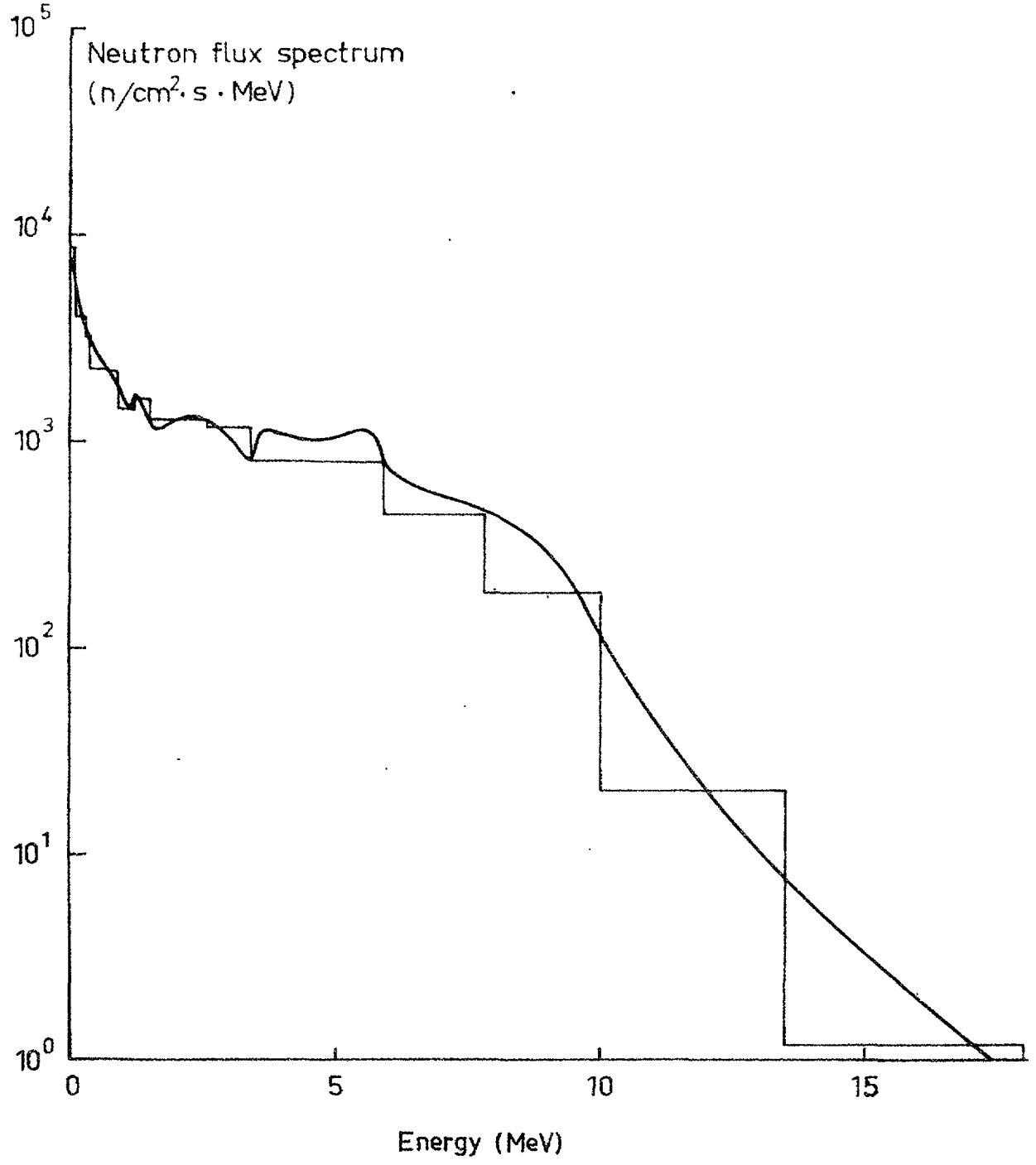

Fig. 4b Med lineär energiskala

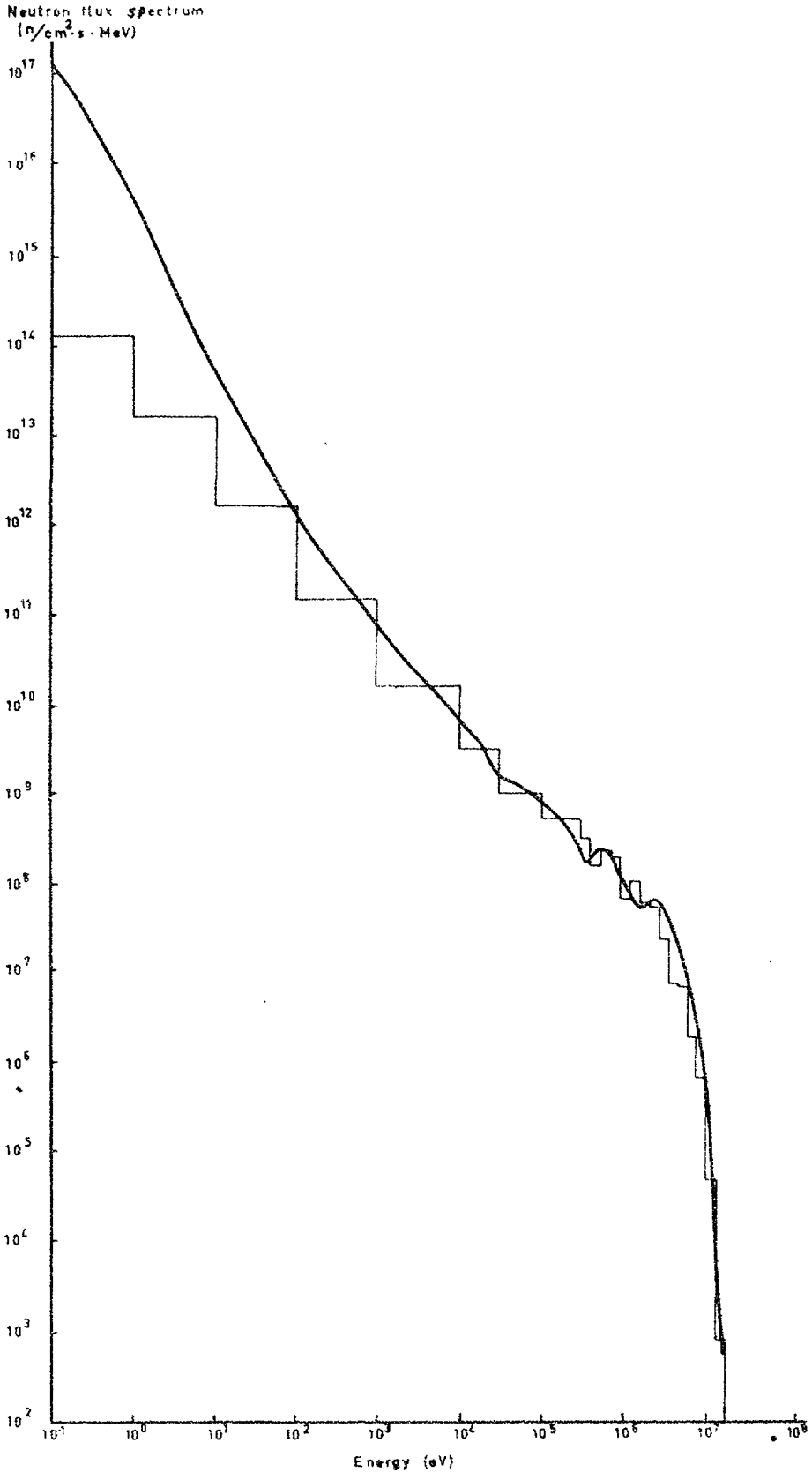

Fig. 5. Neutron flux spectrum at 82 cm in the geometry of fig. 2. Our theoretical result (histogram) is compared with a NIOBE calculation (curve). The deviation at lower energies may be due to an insufficiency in the NIOBE program causing incorrect treatment of the thin aluminum and plastic regions. Experience favors our 1/E dependence for energies < 10 keV. $\mu_o = 0.6$.

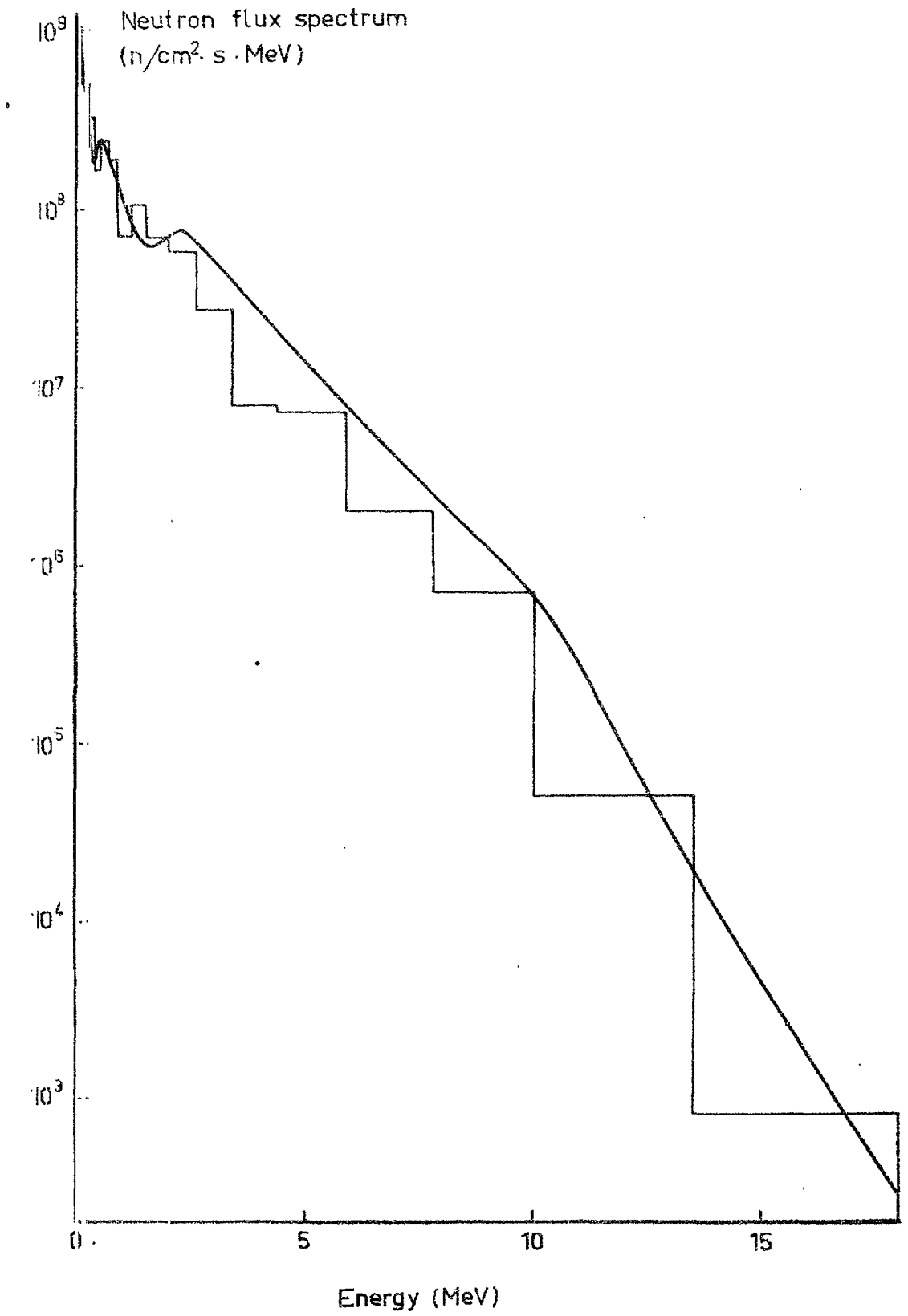

Fig. 5b Med lineär energiskala

LIST OF PUBLISHED AE-REPORTS

1—110. (See the back cover earlier reports.)

111. The paramagnetism of small amounts of Mn dissolved in Cu-Al and Cu-Ge alloys. By H. P. Myers and R. Westin. 1963. 7 p. Sw. cr. 8:—.

112. Determination of the obsolute disintegration rate of Cs^{137}-sources by the tracer method. By S. Hellström and D. Brune. 1963. 17 p. Sw. cr. 8:—.

113. An analysis of burnout conditions for flow of boiling water in vertical round ducts. By K. M. Becker and P. Persson. 1963. 28 p. Sw. cr. 8:—.

114. Measurements of burnout conditions for flow of boiling water in vertical round ducts (Part 2). By K. M. Becker, et al. 1963. 29 p. Sw. cr. 8:—.

115. Cross section measurements of the $^{58}Ni(n, p)^{58}Co$ and $^{2}Si(n, \ _{m})^{26}Mg$ reactions in the energy range 2.2 to 3.8 MeV. By J. Konijn and A. Lauber 1963. 30 p. Sw. cr. 8:—.

116. Calculations of total and differential solid angles for a proton recoil solid state detector. By J. Konijn, A. Lauber and B. Tollander. 1963. 31 p. Sw. cr. 8:—.

117. Neutron cross sections for oluminium. By L. Forsberg. 1963. 32 p. Sw. cr. 8:—.

118. Measurements of smoll exposures of gamma radiation with $CaSO_4$:Mn radiothermoluminescence. By B. Bjärngard. 1963. 18 p. Sw. cr. 8:—.

119. Measurement of gamma radioactivity in a group of contral subjects from the Stockholm area during 1959—1963. By I. Ö. Andersson, I. Nilsson and Eckerstig. 1963. 19 p. Sw. cr. 8:—.

120. The thermox process. By O. Tjälldin. 1963. 38 p. Sw. cr. 8:—.

121. The transistor as low level switch. By A. Lydén. 1963. 47 p. Sw. cr. 8:—.

122. The planning of a small pilot plant for development work an aqueous reprocessing of nuclear fuels. By T. U. Sjöborg, E. Haeffner and Hultgren. 1963. 20 p. Sw. cr. 8:—.

123. The neutron spectrum in a uranium tube. By E. Johansson, E. Jonsson, M. Lindberg and J. Mednis. 1963. 36 p. Sw. cr. 8:—.

124. Simultaneous determination of 30 trace elements in cancerous and noncancerous human tissue samples with gamma-ray spectrometry. K. Samsahl, D. Brune and P. O. Wester. 1963. 23 p. Sw. cr. 8:—.

125. Measurement of the slowing-down and thermalization time of neutrons in water. By E. Möller and N. G. Sjöstrand. 1963. 42 p. Sw. cr. 8:—.

126. Report on the personell dosimetry at AB Atomenergi during 1962. By K.-A. Edvardsson and S. Hagsgård. 1963. 12 p. Sw. cr. 8:—.

127. A gas target with a tritium gas handling system. By B. Holmqvist and T. Wiedling. 1963. 12 p. Sw. cr. 8:—.

128. Optimization in activation analysis by means of epithermal neutrons. Determination of molybdenum in steel. By D. Brune and K. Jirlow. 1963. 11 p. Sw. cr. 8:—.

129. The P_1-approximation for the distribution of neutrons from a pulsed source in hydrogen. By A. Claesson. 1963. 18 p. Sw. cr. 8:—.

130. Dislocation arrangemants in deformed and neutron irradiated zirconium and zircaloy-2. By R. B. Roy. 1963. 18 p. Sw. cr. 8:—.

131. Measurements of hydrodynamic instabilities, flow oscillations and burnout in a natural cirkulation loop. By K. M. Becker, R. P. Mathisen, O. Eklind and B. Norman. 1964. 21 p. Sw. cr. 8:—.

132. A neutron rem counter. By *I. Ö. Andersson and J. Braun.* 1964. 14 p. Sw. cr. 8:—.

133. Studies of water by scattering of slow neutrons. By K. Sköld, E. Pilcher and K. E. Larsson. 1964. 17 p. Sw. cr. 8:—.

134. The amounts of As, Au, Br, Cu, Fe, Mo, Se, and Zn in normal and uraemic human whole blood. A comparison by means neutron activation analysis. By D. Brune, K. Samsahl and P. O. Wester. 1964. 10 p. Sw. cr. 8:—.

135. A Monte Carlo method för the analysis of gamma radiation transport from distributed sources in laminated shields. By M. Leimdörfer. 1964. 28 p. Sw. cr. 8:—.

136. Ejection of uranium atoms from UO_2 by fission fragments. By G. Nilsson. 1964. 38 p. Sw. cr. 8:—.

137. Personell neutron monitoring at AB Atomenergi. By S. Hagsgård and C.-O. Widell. 1964. 11 p. Sw. cr. 8:—.

138. Radiation induced precipitation in iron. By B. Solly. 1964. 8 p. Sw. cr. 8:—.

139. Angular distributions of neutrons from (p, n)-reactions in some mirror nuclei. By L. G. Strömberg, T. Wiedling and B. Holmqvist. 1964. 28 p. Sw. cr. 8:—.

140. An extended Greuling-Goertzel approximation with a P_n -approximation in the angular dependence. By R. Håkansson. 1964. 21 p. Sw. cr. 8:—.

141. Heat transfer and pressure drop with rough surfaces, a literature survey. By A. Bhattachayya. 1964. 78 p. Sw. cr. 8:—.

142. Radiolysis of aqueous benzene solutions. By H. Christensen. 1964. 50 p. Sw. cr. 8:—.

143. Cross section measurements for some elements suited as thermal spectrum indicatars: Cd, Sm, Gd and Lu. By E. Sokolowski, H. Pekarek and E. Jonsson. 1964. 27 p. Sw. cr. 8:—.

144. A direction sensitive fast neutron monitor. By B. Antolkovic, B. Holmqvist and T. Wiedling. 1964. 14 p. Sw. cr. 8:—.

145. A user's manual for the NRN shield design method. By L. Hjärne. 1964. 107 p. Sw. cr. 10:—.

146. Concentration of 24 trace elements in human heart tissue determined by neutron activation analysis. By P. O. Wester. 1964. 33 p. Sw. cr. 8:—.

147. Report on the personnel Dosimetry at AB Atomenergi during 1963. By K.-A. Edvardsson and S. Hagsgård. 1964. 16 p. Sw. cr. 8:—.

148. A calculation of the angular moments of the kernel for a monatomic gas scatterer. By R. Håkanssan. 1964. 16 p. Sw. cr. 8:—.

149. An anion-exchange method far the separation of P-32 activity in neutron-irradited biological material. By K. Samsahl. 1964. 10 p. Sw. cr. 8:—.

150. Inelastic neutron scattering cross sections of Cu^{63} and Cu^{65} in the energy region 0.7 to 1.4 MeV. By B. Holmqvist and T. Wiedling. 1964. 30 p. Sw. cr. 8:—.

151. Determination of magnesium in needle biopsy samples of muscle tissue by means of neutron activation analysis. By D. Brune and H. E. Sjöberg. 1964. 8 p. Sw. cr. 8:—.

152. Absolute El transition probabilities in the dofermed nuclei Yb^{177} and Hf^{179}. By Sven G. Malmskog. 1964. 21 p. Sw. cr. 8:—.

153. Measurements of burnout conditions for flow of boiling water in vertical 3-rod and 7-rod clusters. By K. M. Becker, G. Hernborg and J. E. Flinta. 1964. 54 p. Sw. cr. 8:—.

154. Integral parameters of the thermal neutron scattering law. By S. N. Purohit. 1964. 48 p. Sw. cr. 8:—.

155. Tests of neutron spectrum calculations with the help of foil measurments in a D_2O and in an H_2O-moderated reactor and in reactor shields of concrete and iron. By R. Nilsson and E. Aalta. 1964. 23 p. Sw. cr. 8:—.

156. Hydrodynamic instability and dynamic burnout in natural circulation two-phase flow. An experimental and theoretical study. By K. M. Becker. S. Jahnberg, I. Haga, P. T. Hansson and R. P. Mathisen. 1964. 41 p. Sw. cr. 8:—.

157. Measurements of neutron and gamma attenuation in massive laminated shields of concrete and a study of the accuracy of some methods of calculation. By E. Aalto and R. Nilsson. 1964. 110 p. Sw. cr. 10:—.

158. A study of the angular distributions of neutrons from the Be^{9} (p,n) B^{9} reaction at low proton energies. By. B. Antolkovic', B. Holmqvist and T. Wiedling. 1964. 19 p. Sw. cr. 8:—.

159. A simple opparatus for fast ion exchange separations. By K. Samsahl. 1964. 15 p. Sw. cr. 8:—.

160. Measurements of the Fe^{54} (n, p) Mn^{54} reaction cross section in the neutron energy range 2.3—3.8 MeV. By A. Lauber and S. Malmskog. 1964. 13 p. Sw. cr. 8:—.

161. Comparisons of measured and calculated neutron fluxes in laminated iron and heavy water. By. E. Aalto. 1964. 15. p. Sw. cr. 8:—.

162. A needle-type p-i-n junction semiconductor detector for in-vivo measurement of beta tracer activity. By A. Lauber and B. Rosencrantz. 1964. 12 p. Sw. cr. 8:—.

163. Flame spectro photometric determination of strontium in water and biological material. By G. Jönsson. 1964. 12 p. Sw. cr. 8:—.

164. The solution of a velocity-dependent slowing-down problem using case's eigenfunction expansion. By A. Claesson. 1964. 16 p. Sw. cr. 8:—.

165. Measurements of the effects of spacers on the burnout conditions for flow of boiling water in a vertical annulus and a vertical 7-rod cluster. By K. M. Becker and G. Hernberg. 1964. 15 p. Sw. cr. 8:—.

166. The transmission of thermal and fast neutrons in air filled annular ducts through slabs of iron and heavy water. By J. Nilsson and R. Sandlin. 1964. 33 p. Sw. cr. 8:—.

167. The radio-thermoluminescense of $CaSO_4$: Sm and its use in dosimetry. By B. Bjärngard. 1964. 31 p. Sw. cr. 8:—.

168. A fast radiochemical method for the determination of some essential trace elements in biology and medicine. By K. Samsohl. 1964. 12 p. Sw. cr. 8:—.

169. Concentration of 17 elements in subcellular fractions of beef heart tissue determined by neutron activation analysis. By P. O. Wester. 1964. 29 p. Sw. cr. 8:—.

170. Formation of nitrogen-13, fluorine-17, and fluorine-18 in reactor-irradiated H_2O and D_2O and applicotions to activation analysis and fast neutron flux monitoring. By L. Hammar and S. Forsén. 1964. 25 p. Sw. cr. 8:—.

171. Measurements on background and fall-out radioactivity in samples from the Baltic bay of Tvären, 1957—1963. By P. O. Agnedal. 1965. 48 p. Sw. cr. 8:—.

172. Recoil reactions in neutron-activation analysis. By D. Brune. 1965. 24 p. Sw. cr. 8:—.

173. A parametric study of a constant-Moch-number MHD generator with nuclear ionization. By J. Braun. 1965. 23 p. Sw. cr. 8:—.

174. Improvements in applied gamma-roy spectrometry with germanium semiconductor dector. By D. Brune, J. Dubois and S. Hellström. 1965. 17 p. Sw. cr. 8:—.

175. Analysis of linear MHD power generators. By E. A. Witalis. 1965. 37 p. Sw. cr. 8:—.

176. Effect of buoyancy on forced convection heat tranfer in vertical channels — a literature survey. By A. Bhattacharyya. 1965. 27 p. Sw. cr. 8:—.

177. Burnout data for flow of boiling water in vertical round ducts, annuli and rod clusters. By K. M. Becker, G. Hernborg, M. Bode and O. Eriksson. 1965. 109 p. Sw. cr. 8:—.

178. An analytical and experimental study of burnout conditions in vertical round ducts. By K. M. Becker. 1965. 161 p. Sw. cr. 8:—.

179. Hindered El transitions in Eu^{155} and Tb^{161}. By S. G. Malmskog. 1965. 19 p. Sw. cr. 8:—.

180. Phatomultiplier tubes for low level Cerenkov detectors. By O. Strindehag. 1965. 25 p. Sw. cr. 8:—.

181. Studies of the fission integrals of U235 and Pu239 with cadmium and boron filters. By E. Hellstrand. 1965. 32 p. Sw. cr. 8:—.

182. The handling of liquid waste at the research station of Studsvik, Sweden. By S. Lindhe and P. Linder. 1965. 18 p. Sw. cr. 8:—.

183. Mechanical and instrumental experiences from the erection, commissioning and operation of a small pilot plant for development work on aqueous reprocessing of nuclear fuels. By K. Jönsson. 1965. 21 p. Sw. cr. 8:—.

184. Energy dependent removal cross-sections in fast neutron shielding theory. By H. Grönroos. 1965. 75 p. Sw. cr. 8:—.

185. A new method for predicting the penetration and slowing-down of neutrons in reactor shields. By L. Hjärne and M. Leimdörfer. 1965. 21 p. Sw. cr. 8:—.

Förteckning över publicerade AES-rapporter

1. Analys medelst gamma-spektrometri. Av D. Brune. 1961. 10 s. Kr 6:—.
2. Bestrålningsförändringar och neutronatmosfär i reaktortrycktankar — några synpunkter. Av M. Grounes. 1962. 33 s. Kr 6:—.
3. Studium av sträckgränsen i mjukt stål. Av G. Östberg och R. Attermo. 1963. 17 s. Kr 6:—.
4. Teknisk upphandling inom reaktorområdet. Av Erik Jonson. 1963. 64 s. Kr 8:—.
5. Agesta Kraftvärmeverk. Sammanställning av tekniska data, beskrivningar m. m. för reaktordelen. Av B. Lilliehöök. 1964. 336 s. Kr 15:—.

Additional copies available at the library of AB Atomenergi, Studsvik, Nyköping, Sweden. Transparent microcards of the reports are obtainable through the International Documentation Center, Tumba, Sweden.

EOS-tryckerierna, Stockholm 1965